910 MHz Urban Mobile Radio Propagation: Multipath Characteristics in New York City

DONALD C. COX, SENIOR MEMBER, IEEE

Abstract—Small scale statistics of multipath propagation in a heavily built-up urban mobile radio environment are presented. The statistics cover vehicle travel distances on the order of 30 m along streets. Measuring equipment time delay resolution is about 0.1 μs. In some locations, paths with significant amplitudes are observed with excess delays of 9 to 10 μs. The delay spreads ($\sqrt{\text{second central moment of power delay profile}}$) in this environment are on the order of 2 μs. Often the signal at fixed delays has a Rayleigh-distributed amplitude but large departures from the Rayleigh distribution also occur. From the measurements it appears reasonable to model the urban mobile radio channel as a Gaussian quasi-wide-sense stationary uncorrelated scattering channel within a bandwidth of 10 MHz and for intervals along the street of up to 30 m.

I. Introduction

The characteristics of radio propagation between base stations and mobile vehicles place some of the most fundamental constraints on mobile communication systems. The main features of propagation in the urban mobile radio environment are shadowing of the direct or line-of-sight propagation path by intervening buildings and multipath due to scatter or reflection from buildings surrounding the vehicle [1]-[4]. Vehicle motion produces different Doppler shifts on scatter paths arriving at the vehicle from different angles. The time delays and Doppler shifts associated with the multipath propagation can be measured directly by probing the medium with wide bandwidth pulse or pulse-like transmission.

This paper describes some measured characteristics of multipath propagation at 910 MHz in New York City. The data presented describe the "local" statistics of multipath propagation which cover mobile vehicle travel distances on the order of 30 m. Sets of detailed local statistics such as these for heavily built-up urban areas have not been reported previously in the literature.

II. The Measurements

The measurements were made with a wide-band measuring system that used the correlation properties of pseudorandom shift-register sequences. The system is not a pulse system but the measurements are equivalent to measurements made using short RF pulses. The instrumentation is described in detail in [1].

Manuscript received September 6, 1972.
The author is with Bell Laboratories, Holmdel, N.J. 07733.

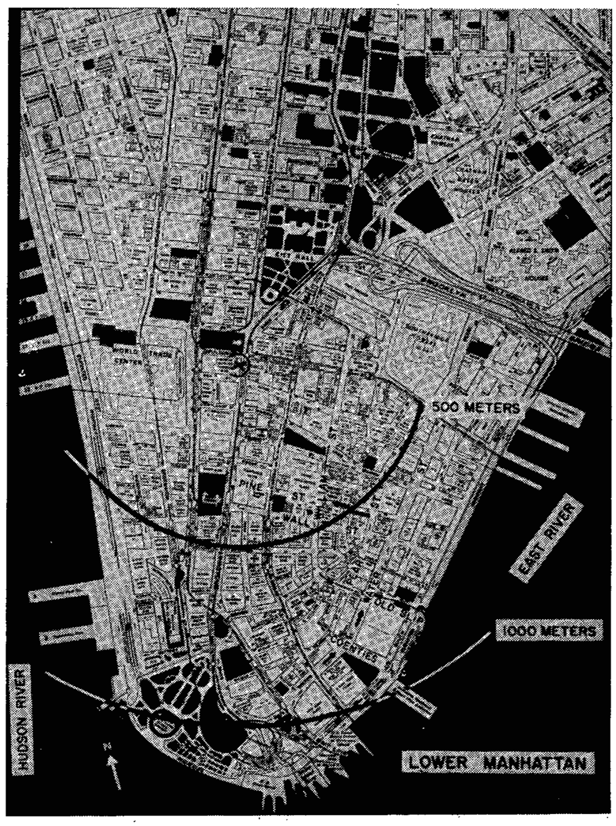

Fig. 1. Map of experimental area on lower Manhattan Island, New York City.

Briefly, a 910 MHz carrier is phase reversal modulated by a pseudorandom shift register sequence and transmitted from an omnidirectional base-station antenna with an elevation beamwidth of about 18°. For these measurements the antenna was located on top of the 120-m high American Telephone and Telegraph building at 195 Broadway, New York City. The transmitter site is marked with an X on the map in Fig. 1. Even though by most standards this is a tall building, it is located in an area where many of the buildings surrounding it are considerably taller. Fig. 2 was taken from the building roof near the transmitting antenna looking toward the financial district (Wall Street, etc.) in the general direction of the streets where the data shown later were taken. It is obvious

Fig. 2. Picture looking towards experimental area in financial district from near the transmitting antenna.

from the picture that the transmitter building is tall relative to the streets but not tall relative to its surroundings.

The receiver is installed in a mobile vehicle (medium size modified Cortez self-propelled mobile home about $2\frac{1}{2}$ meters high) and connected to an omnidirectional $\frac{1}{4}$ wavelength vertical antenna on the roof. The signal received in the vehicle is correlated with a replica of the transmitted signal in two quadrature correlators. The two correlator amplitude outputs in time represent amplitude versus time delay for the low-pass quadrature components, $I(\tau)$ and $Q(\tau)$, of bandpass impulse responses of the propagation path [2]. Since transmitter and receiver logic are both driven from precision frequency standards, the absolute delay reference provided by the synchronizing pulse can be maintained to better than 0.05 μs for a few hours. The range of delays included in one impulse response (the delay window) is 15 μs. This 15 μs window can be moved anywhere within an absolute delay range of 0 to 51.1 μs, which corresponds to path delays of 0 to about 15 Km. The squared envelope of the complex impulse response, $p(\tau) = I^2(\tau) + Q^2(\tau)$, is the same power delay profile $p(\tau)$ which would be received if a triangular pulse with base width of 0.2 μs and a repetition rate of 20 kHz were transmitted through all equipment filters and the propagation medium and detected with a square law detector [1]. The delay resolution of the equipment is about 0.1 μs (10 MHz bandwidth RF signal).

Data that includes complex impulse response components, synchronizing pulses, vehicle speed, etc., were recorded on an analog tape recroder in the mobile vehicle while it was driven at 1.4 m/s along streets on lower Manhattan Island, New York City. These data were then sampled, digitized, and stored on a magnetic disc for computer processing. Data shown later are from Pine Street between Pearl and Williams Streets and from Water Street between Coenties Slip and Old Slip (see Fig. 1). Both street locations have many tall buildings between the transmitting antenna and them, that is, they are behind the tall buildings visible in Fig. 2. Direction of vehicle travel is indicated by the arrows on Fig. 1.

Pine Street is very narrow (10 m between buildings on opposite sides of street) and the tall buildings on both sides form a deep canyon. Water Street is considerably wider (25 m between buildings) but there are many more tall buildings between it and the transmitter. The small-scale statistical data from these streets are representative of data from such heavily built-up areas. The overall average delay spreads obtained probably represent an upper bound on multipath propagation in such an area.

Measurements were made between midnight and about 5:00 A.M. local time when traffic density was low. The most severe scattering centers (longest delays and strongest scattering) are the tall buildings and elevated roadways and these obviously are not affected by traffic. Cars and trucks on the street generally produce only minor multipath effects since they have a relatively small cross section and are also shielded from the transmitting antenna by the large structures. This has been verified in the daytime in heavy traffic. With the receiving vehicle stationary and traffic moving the major features on the power delay profiles remain fixed in delay and amplitude.

Individual Envelope Delay Profiles

The individual envelope delay profiles are plots of received "pulse" (receiver correlation function) amplitude as a function of path delay referred to a fixed absolute delay reference, that is, they are the envelope of the bandpass impulse response of the propagation medium [1], [2] or $\sqrt{p(\tau)}$ where $p(\tau)$ was briefly discussed earlier.

Fig. 3(a) is an envelope delay profile for a line-of-sight path relatively free of multipath propagation. (Data for this profile were taken in a suburban area free of buildings, etc.) It illustrates the equipment resolution and delay window. Fig. 3(b), (c), and (d) are profiles from different locations in New York City, as labeled. The horizontal scales are excess propagation delay in μs from the minimum delay propagation path. The vertical scales are linear in amplitude (voltage). These three profiles are selected bad examples that occur relatively infrequently over relatively short intervals of street. They are not unique however. Note that the paths with long excess delays are of almost equal strength compared to the paths with nearly minimum delay. This is largely due to "fading" of the shorter delay paths at these locations.

Fig. 4 contains three sequences of individual envelope delay profiles taken within a 30 m interval along Pine Street. The profiles in each sequence were taken every 10 cm along the street. Since the delay reference for the measuring system is determined by stable clocks at both the receiver and transmitter and not by triggering on the received signal, the delay measurements are absolute. For the profiles in Fig. 4 the absolute delay to the first arriving "pulse" (the minimum de-

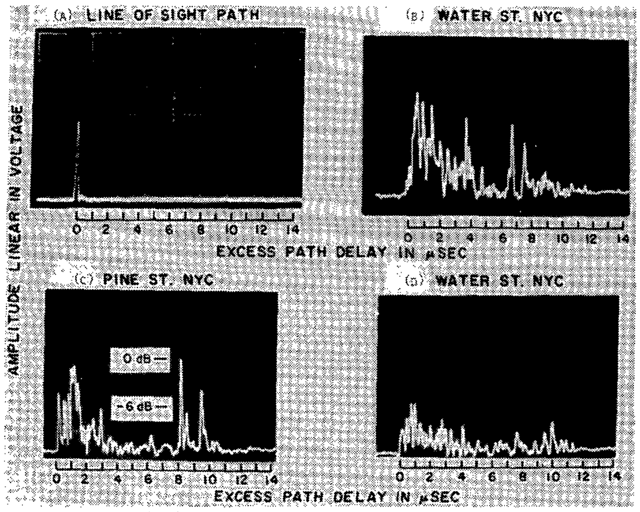

Fig. 3. Individual envelope delay profiles.

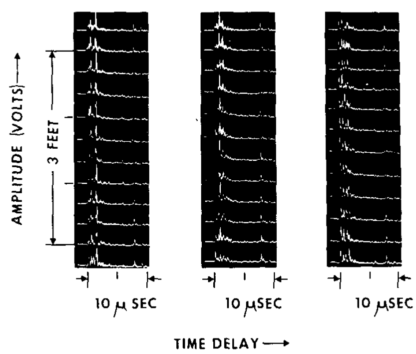

Fig. 4. Three sequences of individual envelope delay profiles from Pine Street.

lay path) is 1.7 μs. Note that the paths near the minimum delay path exhibit deep and rapid fading, indicating the existence of multiple propagation paths within the 0.1 μs resolution of the measurement. For some profiles the strongest path is the minimum delay path but for many others it is a path with excess delay of up to about 1.5 μs. The paths with excess delays of 8 to 9 μs are relatively stable.

Average Power Delay Profiles

Sampled individual power delay profiles $p_i(\tau_k)$ were computed by $p_i(\tau_k) = I_i^2(\tau_k) + Q_i^2(\tau_k)$ where the i orders the set of profiles along the street and k orders the delay samples of each profile. A specified delay τ_k is the same propagation delay from transmitter to receiver for all profiles of a given profile set. The profiles shown in the previous figures were plots of individual $p_i(\tau)$ for various values of i.

An average power delay profile $P(\tau_k)$ for a set of N consecutive individual profiles is then computed as

$$P(\tau_k) = \frac{1}{N} \sum_{i=1}^{N} p_i(t_k) = \langle |h(\tau_k)|^2 \rangle i,$$

where $h(\tau_k)$ is the bandpass impulse response discussed in [2].

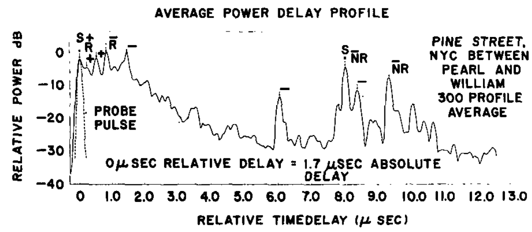

Fig. 5. Average power delay profile from Pine Street.

These profiles can be described by several parameters. The center of gravity or first moment of the profile with respect to the first arrival delay is a measure of the average excess delay D_e. Average excess delay is calculated by

$$D_e \triangleq \frac{\sum_{k=1}^{M} \tau_k P(\tau_k)}{\sum_{k=1}^{M} P(\tau_k)} - \tau_A,$$

where M is the index of the last sample along the delay axis which has a significant amplitude and $k = 1$ is a point before the minimum arrival delay τ_A at which the profile amplitude is insignificant. The locations of $k = 1$ and M are chosen so that moving the $k = 1$ point to smaller delay values or moving the last sample to larger delay values does not affect the value of D_e. Average excess delay is related to the average ranging error that would occur in narrowband CW phase ranging systems [5].

The square root of the second central moment is one possible measure of the delay spread S or width of a power delay profile. It is calculated

$$S \triangleq \sqrt{\frac{\sum_{k=1}^{M} (\tau_k - D_e)^2 P(\tau_k)}{\sum_{k=1}^{M} P(\tau_k)}},$$

where the parameters are as defined previously. Other measures of width, such as delay between outer −3 dB or −10 dB points are also useful from some profiles. Delay spread sets limits on many communication system performance parameters, as indicated in [1].

Fig. 5 is an average power delay profile from Pine Street, New York City. The horizontal axis is excess delay with the zero set at approximately the minimum delay path which is an absolute delay of 1.7 μs. This profile is the average of 300 consecutive individual profiles, including those in Fig. 4, covering about 30 m of travel along the street. The vertical scale is linear in dB relative to the maximum. The total power received from paths with excess delay less than 1.5 μs is much greater than that from paths with excess delays of 8 to 10 μs. Thus the effects of these extreme paths will not be as great on the average as would be the case for nearly equal received powers at 0 and 9 μs excess delays. This fact is further illustrated by the delay spread of 2.5 μs for this profile (see

TABLE I

Profile Location	Average Excess Delay (μs)	Average Absolute Delay (μs)	Minimum Absolute Delay (μs)	Delay Spread S (μs)	Profile Width −3 dB (μs)	Profile Width −10 dB (μs)	Number of Profiles Averaged
Pine Street	1.9	3.6	1.7	2.53	1.5	9.6	300
Water Street, 1	1.6	4.3	2.7	1.95	0.14	3.3	270
Water Street, 2	2.4	5.3	2.9	2.19	0.8	7.4	270

Table I). (Two discrete equal strength paths with excess delays of 0 and 9 μs would have a delay spread of 4.5 μs.)

The average power delay profile in Fig. 6 is an average of 270 consecutive individual profiles covering a 27 m interval along Water Street. The excess delay axis 0 is at an absolute delay of 2.72 μs.

Table I summarizes the characteristics of the profiles in Figs. 5 and 6 along with another one from a nearby location, 2, on Water Street. Absolute delay is calibrated to about ±0.1 μs.

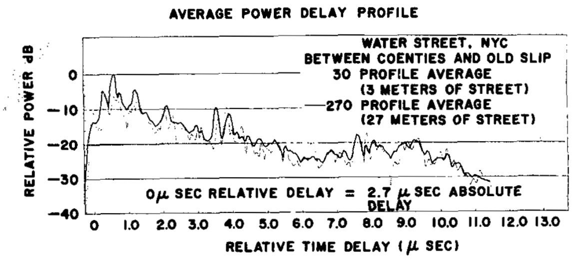

Fig. 6. Average power delay profile from Water Street.

Cumulative Distribution of Signal Level at Fixed Delays

The amplitude at fixed delays for a series of individual envelope delay profiles, such as in Fig. 4, is observed to fluctuate (to fade) from profile to profile. This fading was also observed in profiles taken at 910 MHz in suburban areas [1] and in urban areas at 450 MHz with wider (1/2 μs) probing pulses [3] and is attributed to unresolved multiple propagation paths. The actual distributions of signal level at several fixed delays for the 300 profiles whose average profile is Fig. 5 are plotted in Fig. 7. The solid straight line in Fig. 7 is for a Rayleigh distribution. The distributions for the signals at 0 μs and 0.82 μs approximate a Rayleigh distribution within about 2 dB over a 30 dB range. The paths with excess delays of 8.02 and 9.34 μs are relatively stable with total amplitude fluctuation of less than 15 dB (less than 10 dB at 9.34 μs). On Fig. 5 the symbols ○, ●, □, and ■ and the letters R or NR refer the data at the indicated delays to the distributions on Fig. 7. The R and NR indicate Rayleigh and non-Rayleigh distributed signal fluctuations, respectively. The row of open squares at 99.67 percent on Fig. 7 are quantization effects due to the small finite sample (299 samples out of 300 is 99.67 percent).

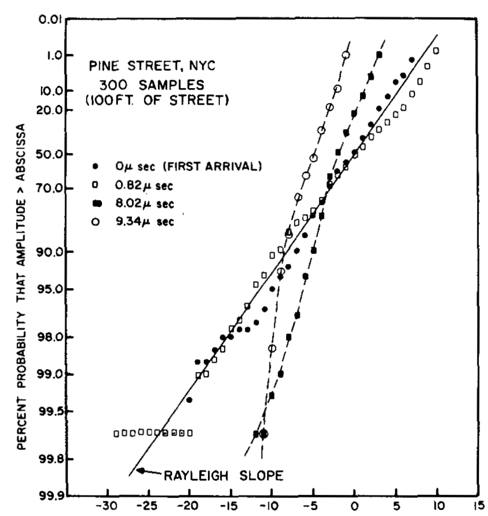

Fig. 7. Cumulative signal level distributions at fixed delays from Pine Street.

Doppler Spectra at Fixed Delays

Scattered signals arriving at the measuring vehicle will be Doppler shifted by different amounts depending on the angle that the arrival path makes with the direction of vehicle travel [8]. When the Doppler shift is expressed in units of cycles/m of vehicle travel, it is not dependent on actual vehicle velocity. (Conversion to units of Hz requires only multiplication by vehicle velocity in m/s.) Signals arriving from scatters directly ahead of the vehicle will be shifted higher in frequency (positive) by the maximum amount $1/\lambda$ where λ is the wavelength of the signal; those directly behind will be shifted negatively by the same amount.

Since the equipment used in this experiment uses quadrature coherent detection and stable frequency references, the RF carrier Doppler shifts associated with various scatter paths can be measured. This Doppler shift information is useful in communication system analysis and for further resolving the multipath structure of the media, since paths having nearly the same time delay can be separated if they arrive from different angles. For example, if an adaptive equalizer were built to equalize the multipath on a mobile radio channel for wideband digital data, the bandwidth of the data signal and the spread in time delays of the paths would determine the number of taps required on the equalizer but the Doppler shifts associated with the paths determine the rate at which the tap gains must be adjusted, i.e., the equalization rate required.

Fig. 8(a) is the RF Doppler spectrum of the signal at the fixed excess delay of 0 μs for the 30 m of street represented in Fig. 5. It was obtained by complex Fourier transforming the measured $I_i(\tau)$ and $Q_i(\tau)$ samples at 0 μs delay for $i = 1$ to 300 after they had been multiplied by a Hamming window to reduce spectrum sidelobes. The lower horizontal scale is fre-

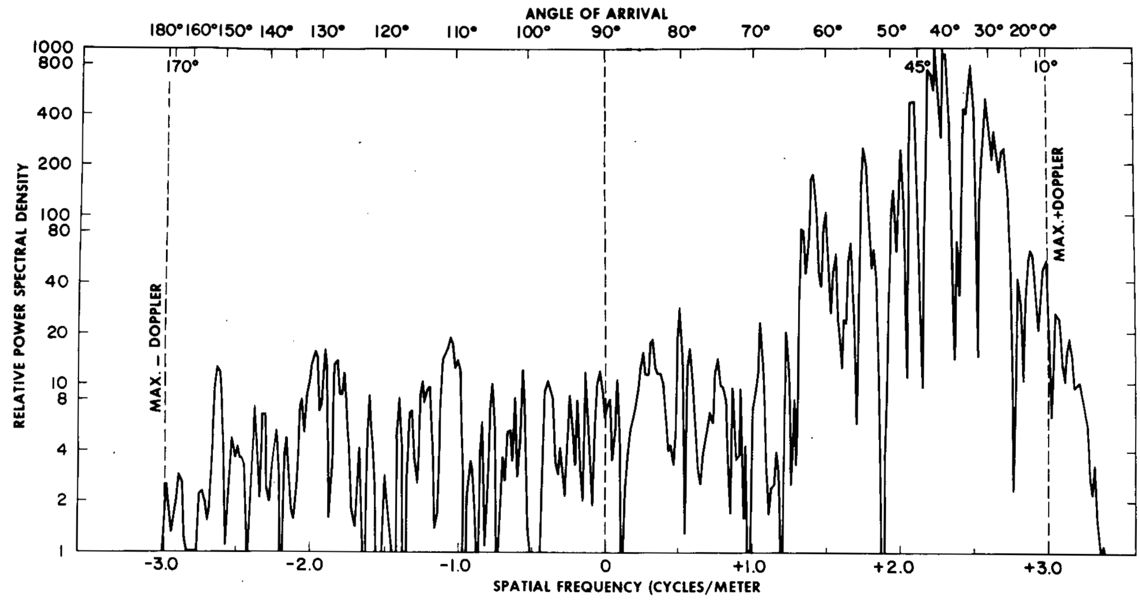

(a)

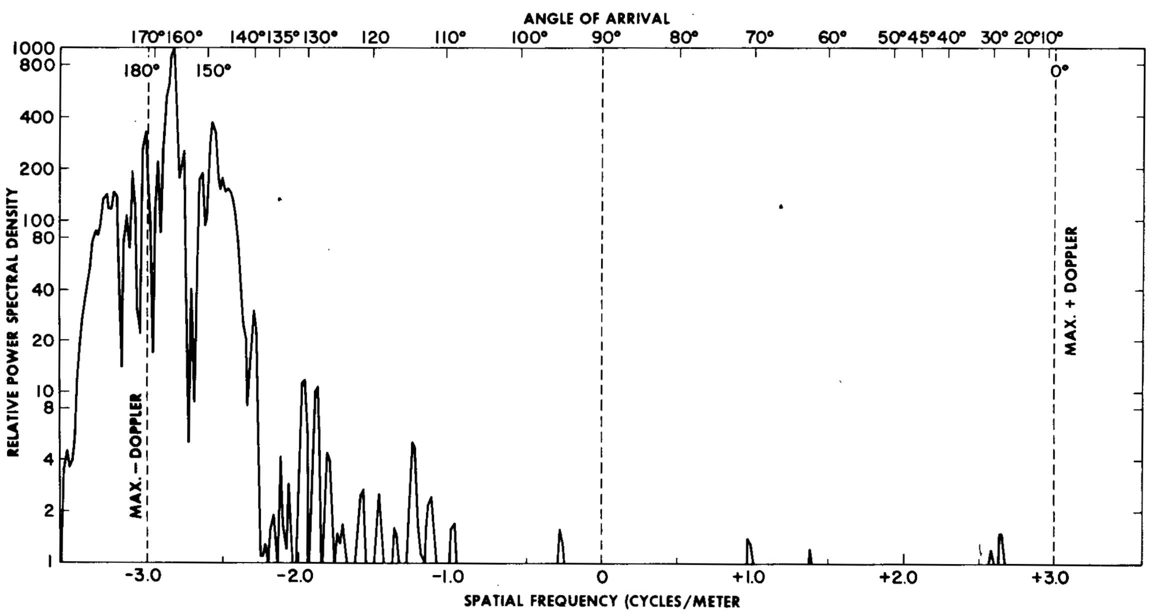

(b)

Fig. 8. (a) RF Doppler spectrum at 0 μs excess delay on Pine Street. (b) RF Doppler spectrum at 8.02 μs excess delay on Pine Street.

quency offset from center frequency (910 MHz) in cycles/m of travel. The approximate maximum possible plus and minus shifts are indicated by the vertical dashed lines. The vertical scale is a logarithmic relative power scale. Since the Doppler frequency shift is proportional to the cosine of the angle of arrival of the incoming wave referred to the direction of vehicle travel, the frequency scale can be converted to an angle of arrival scale. This angle of arrival scale is the upper horizontal scale on the figure. The angle specifies a cone only so it is not possible to differentiate between paths arriving from the right or left. Noise and spurious responses are about 30 dB below the spectral maximum. Hamming window sidelobes are about 40 dB below the maximum. Vehicle velocity could not be held constant within the spectrum resolution of the sample and the equipment frequency stability. The general "multiple peaked" nature of the overall spectral peaks is due to discontinuities in measuring vehicle velocity which result from irregularities in the street surface.

Fig. 8(b) is the equivalent RF Doppler spectrum at 8.02 μs delay. The relative power scale is referred to the same level as

Fig. 8(a). At 8.02 μs the average received power is about 2.3 dB below the average received power at 0 μs (see Fig. 5) but the maximum value of the two spectra [Fig. 8(a) and (b)] are nearly the same. These observations are not inconsistent because there is a significant amount of power spread out over a relatively large frequency range at 0 excess delay but at 8.02 μs the power is very concentrated in frequency. The total power integrated over the entire Doppler range can be greater then even though the maxima are equal. Spectra at other delays have different maximum values. Independent accurate measurement of vehicle velocity, recorded simultaneously with the data, indicate that changes of velocity on the order of that required to produce the broadening of one peak into the jagged series of peaks near the maximum negative Doppler shift in Fig. 8(b) did occur during the data run.

On Fig. 5, the letter S above the profile at 0 and 8 μs indicates the position of these spectra on the delay profile. The associated + and - indicate the direction (+ is up in frequency) of the frequency shift of the strongest peak in the Doppler spectrum at that delay. The + and - signs and arrows at other delays on Fig. 5 indicate the direction of shift of the strongest peak for spectra not included in this paper.

It is interesting to speculate on the sources of reflection or scatter that produce the dominant features on a power profile, taking into account the map (Fig. 1), knowledge of the environment, and the RF Doppler spectra. For example, at excess delays of 0 to about 0.5 μs in Fig. 5 most of the energy arrives from ahead of the vehicle (+ Doppler shift). This energy is "forward" scattered or reflected from buildings ahead of the vehicle. The weakness of the signal at 0 excess delay, the severe shadowing of the vehicle on Pine Street, and the fact that the measured absolute delay appears slightly greater than the map distance to the street suggest that this minimum delay path is also due to reflection from a building ahead of and very close to the vehicle. Most of the energy from 0.8 μs on out in excess delay comes from directly behind the vehicle (approximately maximum negative Doppler shift). This is consistent with the fact that the end of Pine Street is blocked off by buildings at Broadway so that single reflection paths with excess delays greater than 0.7 μs are not possible from ahead of the vehicle. Backscatter from buildings between the vehicle and the East River accounts for the paths between 0.5 and 1.5 μs. A single reflection path from structures along the East River first occurs at about 1.5 μs excess delay. Thus, the decrease in scattered power from 1.5 μs to about 8 μs is caused by the East River open area. Note also that even if Pine Street were not blocked off at Broadway, this decrease of scattered power would probably occur because the Hudson River open area would start at about 2.0 μs. Paths in the 2 to 6 μs region are probably due to multiple reflections. The strong paths near 8 μs excess delay correspond to the first reflections from the "leading edge" of Brooklyn. The near maximum negative Doppler shift indicates that the energy reflected from Brooklyn is traveling straight down the street from behind the vehicle. Paths with greater than 8 μs excess delay result from tall structures further along the waterfront or back from the water in Brooklyn. The relatively strong path at 6 μs does not correspond to any known structure in the East River. It could be caused by a ship but is more likely due to multiple reflections.

III. Conclusions

Small scale statistics of multipath propagation at 910 MHz in a heavily built-up area have been presented. In some locations paths with significant amplitudes are observed with excess delays of 9 to 10 μs. The delay spreads ($\sqrt{\text{second central moment of power delay profile}}$) for these areas are 2 to $2\frac{1}{2}$ μs. For excess delays up to 1 or 2 μs considerable energy arrives, via paths at different angles to the vehicle, which cannot be resolved by the 0.1 μs resolution probe. This results in envelope fading at fixed excess delays as the vehicle moves along a street. The fading is approximately Rayleigh distributed. Although the inference is not unique [6] the Rayleigh-distributed envelope suggests modeling of the process as a Gaussian random process. Correlation of the fading envelope at different excess delays has not been computed but visual inspection of sequences of individual envelope delay profiles suggests that the correlation is very low. Also, the Doppler spectra at different delays are quite different. All Doppler spectra cutoff abruptly at spatial frequencies of $\pm 1/\lambda$. Thus, from the results of the delay and Doppler measurements it appears reasonable to model the urban mobile radio channel as a Gaussian quasi-wide-sense stationary uncorrelated scattering channel [7], at least within a bandwidth of 10 MHz and for intervals along a street of up to 30 m. Usually for intervals of over 50 to 100 m of travel along a street the multipath scattering process becomes grossly nonstationary as dominant scatterers and shadowing features (buildings, etc.) change. It appears that joint distributions of average received power and delay spread for a collection of average power delay profiles would be useful in computing system performance on a statistical basis over a large area.

Acknowledgment

The author would like to thank W. E. Legg, A. J. Rustako, R. M. Murray, and C. O. Stevens for their help in taking the data in New York City and W. E. Legg for his help in the data reduction.

References

[1] D. C. Cox, "Delay Doppler characteristics of multipath propagation at 910 MHz in a suburban mobile radio environment," *IEEE Trans. Antennas Propagat.*, vol. AP-20, pp. 625-635, Sept. 1972.
[2] —, "Time and frequency domain characterizations of multipath propagation at 910 MHz in a suburban mobile radio environment," *Radio Sci.*, Dec. 1972.
[3] W. R. Young, Jr. and L. Y. Lacy, "Echoes in transmission at 450 megacycles from land-to-car radio units," *Proc. IRE*, vol. 38, pp. 255-258, Mar. 1950.
[4] G. L. Turin, F. D. Clapp, T. L. Johnston, S. B. Fine, and D. Lavry, "A statistical model of urban multipath propagation," *IEEE Trans. Veh. Technol.*, vol. VT-21, pp. 1-9, Feb. 1972.
[5] J. S. Engel, "Effects of multipath transmission on the measured propagation delay of an FM signal," *IEEE Trans. Veh. Technol.*, vol. VT-18, pp. 44-52, May 1969.
[6] S. H. Lin, "The cumulative amplitude distributions of fading signals," presented at the U.S. Nat. Comm. of URSI 1971 Spring

Meeting, Apr. 8-10, 1971, Washington, D.C., paper 2-3, Commission II.
[7] P. A. Bello, "Characterization of randomly time-variant linear channels," *IEEE Trans. Commun. Syst.*, vol. CS-11, pp. 360-393, Dec. 1963.
P. A. Bello and B. D. Nelin, "Optimization of subchannel data rate in FDM-SSB transmission over selectively fading media," *IEEE Trans. Commun. Syst.*, vol. CS-12, pp. 46-53, Mar. 1964.
[8] D. C. Cox, "A measured delay-Doppler scattering function for multipath propagation at 910 MHz in an urban mobile radio environment," *Proc. IEEE* (Lett.), vol. 61, pp. 479-480, Apr. 1973.

Donald C. Cox (S'58-M'61-SM'72) was born in Lincoln, Neb., on November 22, 1937. He received the B.S. and M.S. degrees from the University of Nebraska, Lincoln, in 1959 and 1960, respectively, and the Ph.D. degree from Stanford University, Stanford, Calif., in 1968, all in electrical engineering.

From 1960 to 1963 he was a Lieutenant in the U.S. Air Force working on microwave communications system design for the Dyna-Soar project at Wright-Patterson Air Force Base, Ohio. From 1963 to 1968 he was at Stanford University, first as a Research Assistant and later as a Research Associate, working on tunnel diode amplifier design and on research in microwave propagation in the troposphere. Since 1968 he has been a Member of the Technical Staff of Bell Laboratories, Holmdel, N.J., doing research in propagation in the urban mobile radio environment and on high capacity mobile radio systems.

Dr. Cox is a member of Commission II of USNC/URSI, Sigma Xi, Sigma Tau, Eta Kappa Nu, and Pi Mu Epsilon and is a Registered Professional Engineer in the states of Ohio and Nebraska.

The Elevation Angle of Mobile Radio Signal Arrival

WILLIAM C.-Y. LEE, MEMBER, IEEE, AND ROBERT H. BRANDT

Abstract—**Field measurements of mobile radio signals have shown that signal arrival is concentrated in elevation angles lower than 16°. This suggests use of an omnidirectional antenna with vertical directivity, instead of the usual whip antenna, to increase average signal strength as a further improvement in the advantages of diversity reception.**

I. INTRODUCTION

FOR a long time mobile radio engineers have tried hard to find ways to reduce signal fading and increase average signal strength. As we know, all kinds of diversity schemes can meet the above requirements and give a certain improvement in signal. Now in addition to the diversity schemes, there are some other ways that reduce the signal fading or increase the signal strength. Several years ago, Lee [1] investigated the mobile radio signal fading from a directional antenna with different azimuthal half-power beamwidths of 45°, 26°, and 13.5°. He found that using directional antennas did help in reducing the signal fading, but not in increasing the average signal strength, as the half-power beamwidth of the directional antenna became narrower. The reason for no improvement in the average signal strength was that the directions of the mobile radio signal arrival at the mobile antenna were more or less uniformly distributed in the horizontal plane. It turned out that the greater the directivity of the antenna, the smaller the portion of the incoming signal received. Hence no increase in the average signal strength was obtained. Is there some other kind of antenna that can be used to increase the average signal strength in a diversity scheme to gain additional signal strength? Before answering this question we should investigate the elevation angle of arrival of mobile radio signals while the mobile unit is moving on the streets. We would like to know if the signal arrival is concentrated in a narrow elevation angle above the horizontal. If so, we may use an omnidirectional antenna with vertical directivity (which suppresses high angle radiation) pointing horizontally in order to increase the average signal strength. This is the aim of this paper.

Manuscript received June 19, 1972. This paper was presented at the Microwave Mobile Radio Symposium, Department of Commerce Laboratories, Boulder, Colo., Mar. 1-3, 1972.
The authors are with Bell Laboratories, Holmdel, N.J. 07733.

II. ANALYSIS

For investigating the elevation angle of signal arrival, we may use any omnidirectional antenna with vertical directivity in which gain is referred to the whip antenna. Then we observe the mobile radio signals received from the vertical-directivity antenna and the whip antenna while the mobile unit is moving. If there is no difference in the signal strengths between two antennas, it means that the signal arrival is uniformly spread over the elevation angles. It can be seen as the vertical directivity of the antenna is increased, the proportion of signal received from higher elevation angles is reduced. Hence no in-